AD-A047 806 NAVAL RESEARCH LAB WASHINGTON D C F/G 18/1
RAYLEIGH-TAYLOR INSTABILITY IN A LAYERED LASER-DRIVEN TARGET.(U)
SEP 77 F S FELBER

UNCLASSIFIED NRL-MR-3506 SBIE-AD-E000 027 NL

1 OF 1
AD A047806

END
DATE FILMED
1-78
DDC

(13) NW

NRL Memorandum Report 3506

Rayleigh-Taylor Instability in a Layered Laser-Driven Target

F. S. FELBER

Laser Plasma Branch
Plasma Physics Division

September 1977

NAVAL RESEARCH LABORATORY
Washington, D.C.

SECURITY CLASSIFICATION OF THIS PAGE (When Data Entered)

REPORT DOCUMENTATION PAGE

READ INSTRUCTIONS BEFORE COMPLETING FORM

1. REPORT NUMBER: NRL Memorandum Report 3506	2. GOVT ACCESSION NO. (14)
3. RECIPIENT'S CATALOG NUMBER: NRL-MR-3506	
4. TITLE (and Subtitle): RAYLEIGH-TAYLOR INSTABILITY IN A LAYERED LASER-DRIVEN TARGET. (6)	5. TYPE OF REPORT & PERIOD COVERED: Interim report on a continuing NRL problem. (9)
	6. PERFORMING ORG. REPORT NUMBER
7. AUTHOR(s): F.S. Felber* (10)	8. CONTRACT OR GRANT NUMBER(s)
9. PERFORMING ORGANIZATION NAME AND ADDRESS: Naval Research Laboratory, Washington, D.C. 20375 — LPN	10. PROGRAM ELEMENT, PROJECT, TASK AREA & WORK UNIT NUMBERS: NRL Problem H02-29A; PE ERDA
11. CONTROLLING OFFICE NAME AND ADDRESS: Energy Research and Development Administration, Washington, D.C. 20545 (11)	12. REPORT DATE: Sep[redacted]977
	13. NUMBER OF PAGES: 21
14. MONITORING AGENCY NAME & ADDRESS(if different from Controlling Office) (12) 21 p.	15. SECURITY CLASS. (of this report): UNCLASSIFIED
	15a. DECLASSIFICATION/DOWNGRADING SCHEDULE

16. DISTRIBUTION STATEMENT (of this Report)

Approved for public release; distribution unlimited.

ERDA Letter S-10-77-0018

17. DISTRIBUTION STATEMENT (of the abstract entered in Block 20, if different from Report)

(18) SBIE (19) AD-E000 027

18. SUPPLEMENTARY NOTES

*This work was supported by a National Research Council Resident Research Associateship at the Naval Research Laboratory.

19. KEY WORDS (Continue on reverse side if necessary and identify by block number)

Rayleigh-Taylor
Instability
Layered targets
Laser-driven targets
Pellet design
Inhomoegeneous laser targets

20. ABSTRACT (Continue on reverse side if necessary and identify by block number)

Growth rates of Rayleigh-Taylor modes, particularly those of long wavelength, are reduced at fluid interfaces in inhomogeneous laser-driven targets by the density gradients occurring naturally as a result of the acceleration. Growth rates can be reduced further by interposing layers of intermediate density at unstable interfaces between layers of high and low density, and by fabricating target layers with favorable density gradients between discontinuities. An approximate closed form expression for the growth rate of fluid instabilities in a multi-layered laser-driven target is presented.

DD FORM 1 JAN 73 1473 EDITION OF 1 NOV 65 IS OBSOLETE
S/N 0102-014-6601

SECURITY CLASSIFICATION OF THIS PAGE (When Data Entered)

251 950

CONTENTS

RAYLEIGH-TAYLOR INSTABILITY IN A LAYERED LASER-DRIVEN TARGET

I. INTRODUCTION

The Rayleigh-Taylor[1] instability arises in the acceleration of a fluid by one of lower density. Although this instability has not yet been observed in a laser-driven plasma, it is expected to represent a major obstacle to achieving laser-induced fusion for the following reason. Necessary to induce a fusion reaction in a spherical pellet is a high compression of the pellet. A pellet can be highly compressed only if it retains sufficient symmetry during implosion. The Rayleigh-Taylor instability can cause corrugations in the hydrodynamic flow to grow nonlinearly to form bubbles and spikes.[2]

There are several surfaces in a laser-driven plasma at which the growth of Rayleigh-Taylor instability is potentially large. One such surface is the ablation layer separating the cold, high density fluid from the hot, low density material blown off by the heat conducted inwards from the region of laser energy deposition. Another such surface is the critical surface, where deposition of laser momentum can cause steep density gradients.[3,4] If the laser target is inhomogeneous, consisting of strata of different materials, then growth of the instability can be large at any fluid interface where the acceleration is directed towards the denser material.

Several stabilizing mechanisms for the Rayleigh-Taylor instability are well known. Viscosity can reduce the growth rate of short wavelength perturbations,[5] as can heat flux.[6] Convection of material through a decreasing density gradient can help stabilize it.[7] Firepolishing is another possible stabilizing mechanism whereby the peaks of density corrugations at the ablation surface, being closer to

Note: Manuscript submitted August 10, 1977.

the heat source, ablate faster than the troughs.[7] Because a shock acceleration causes linear rather than exponential growth of a perturbation,[8] a series of shocks may give a sufficiently low growth factor to successfully implode a pellet if excessive heating and burn-through of the pellet can be avoided. A novel related possibility is stabilization of the ablation surface by "shaking" it with an oscillating laser deposition[9] in the same way that an inverted pendulum can be stabilized by oscillating its base. Since gradual density gradients are less unstable than steep gradients,[5] methods have been proposed for reducing the density gradient at the ablation surface.[10]

Although much research has been applied to the study of the Rayleigh-Taylor instability in laser-driven plasmas, the results are as yet inconclusive. Analytic models of the roles of relevant stabilizing mechanisms are rare.[7,11] The results of numerical simulation studies of fluid instability in laser-fusion pellets are inconsistent and even conflicting.[12-15]

Most studies of Rayleigh-Taylor instability in laser-driven targets have been concerned with homogeneous targets. Inhomogeneous pellets have been considered candidates for laser fusion for some time.[16-19] However, recent claims from the Lebedev Physics Institute[20-21] suggest that certain inhomogeneous hollow pellets with very thin shells of aspect ratio $R/\Delta R \approx 100$ can be imploded to yield an energy gain of as much as 10^3. The Lebedev shell design calls for a high density material, such as lead or gold, to be sandwiched between low density deuterium-tritium fuel layers on the inside and a moderate density ablator, such as plastic or beryllium, on the outside. In this design the interface between the dense layer and the ablator is unstable in the absence of stabilizing mechanisms. The Lebedev results, if valid, suggest that stabilizing mechanisms operate at this interface. In this paper one possible stabilizing mechanism for material interfaces in laser-driven targets is presented.

In an earlier paper[4] a global model of a flat laser-driven target was presented. This model is extended in the next section to include

inhomogeneous slabs, and provide the basic, unperturbed state from which the linear instability analysis of Section III proceeds. The result of the instability analysis is that density gradients established in a slab by acceleration reduce the growth rate of the Rayleigh-Taylor instability at an unstable discontinuity in the unablated material. The reduced growth rate is calculated. In Section IV the calculation of growth rate is generalized to apply to any number of layers in a laser-driven slab, and it is suggested that further reduction of instability can be achieved by interposing layers of intermediate density between the ablator and high-density layer. An analytic expression for the growth rate of a perturbation in a multi-layered target is derived. To illustrate the stabilizing effect of intermediate-density layers, an example is presented in which the reduced growth rate is calculated as a function of the width of an intermediate layer.

II. BASIC STATE

The system of 2-D fluid equations to be used in the following instability analysis consists of the continuity equation

$$\frac{\partial \rho}{\partial t} = - \frac{\partial}{\partial x} (\rho v_x) - \frac{\partial}{\partial y} (\rho v_y) \quad , \tag{1}$$

momentum equations

$$\frac{\partial}{\partial t} (\rho v_x) = - \frac{\partial}{\partial x} (P + \rho v_x^2) - \frac{\partial}{\partial y} (\rho v_x v_y) + \rho g \tag{2}$$

$$\frac{\partial}{\partial t} (\rho v_y) = - \frac{\partial}{\partial y} (P + \rho v_y^2) - \frac{\partial}{\partial x} (\rho v_y v_x) \quad , \tag{3}$$

energy equation

$$\frac{\partial E}{\partial t} = - \frac{\partial}{\partial x} [(E + P) v_x + q_x] - \frac{\partial}{\partial y} [(E + P) v_y + q_y] + \rho g v_x \tag{4}$$

and the equation of state

$$P = \rho T/m \quad . \tag{5}$$

Here $v_x\hat{x} + v_y\hat{y}$ is the velocity of a volume element of mass density ρ, temperature T in energy units, pressure P, ion mass m, and local energy density $E = (3P + \rho v_x^2 + \rho v_y^2)/2$. Following Spitzer,[23] we take the heat flux to be

$$q_x = -\frac{K_o}{Z} T^{5/2} \frac{\partial T}{\partial x} \quad , \qquad q_y = -\frac{K_o}{Z} T^{5/2} \frac{\partial T}{\partial y} \quad , \tag{6}$$

with Z the atomic number, and K_o considered constant, its weak temperature, density, and Z dependence ignored.

In a reference frame accelerating with the fluid such that the ablation front is at rest in this frame, the effective gravity in the positive x direction is constant g. In this accelerating reference frame the temperature and density profiles of a slab appear stationary (except near the ends of the slab), and a steady state model provides a good description of the slab over times short compared to v_{max}/g, in which v_{max} is the supersonic fluid velocity occurring at the outer edge of the ablation.[4]

In Reference 4 the fluid equations were used to formulate a global steady state model of a slab accelerated by a laser; the acceleration and boundaries of the slab were determined self consistently. A portion of a typical slab satisfying the steady state fluid equations is shown in Fig. 1. This slab consists of two fluids, with fluid I having a greater ion mass, atomic number, and density than fluid II. The ablation layer, occurring in fluid II, is that region to the right of the surface of maximum density at $x = x_a$ containing the steep density gradient. To the left of the ablation layer, the gentle pressure and density gradients are described by the approximate analytic solutions to the steady state fluid equations[4]

$$
\begin{aligned}
P &\approx P(x_a)\,[1 + \rho(x_a) g x / P(x_a)] \\
\rho &\approx \rho(x_a)\,[1 + 3\rho(x_a) g x / 5P(x_a)] \\
v_x &\approx v(x_a)\,[1 - 3\rho(x_a) g x / 5P(x_a)] \quad , \quad v_y = 0 \quad , \\
q_x &\approx -\frac{2}{5}\, mg\, \frac{K}{Z}\, T^{5/2}(x_a) \quad , \quad q_y = 0 \, .
\end{aligned}
\tag{7}
$$

If we transform to a frame of reference at rest with respect to the fluid interface at $x = 0$, the density and pressure profiles are no longer steady. In this new reference frame

$$
\begin{aligned}
P &\approx P_i\,[1 + \rho_i g (x + v_i t)/P_i] \\
\rho &\approx \rho_i\,[1 + 3\rho_i g (x + v_i t)/5P_i] \\
v_x &\approx v_i(-3\rho_i g x / 5P_i) \quad , \quad v_y = 0 \\
q_x &\approx -\frac{2}{5}\, m_i g\, \frac{K_o}{Z}\, T_i^{5/2} \quad , \quad q_y = 0 \quad .
\end{aligned}
\tag{8}
$$

The index i has the value 1 or 2 depending on whether the quantity is evaluated to the left or right of the fluid interface respectively.

Since the heat flux is a small constant, and the fluid quantities satisfy an adiabatic gas law, $P\rho^{-5/3} \approx P_i \rho_i^{-5/3}$, it may be supposed that heat conduction will be of negligible importance in a consideration of instability at the cold fluid interface. However, the energy equation (4) does yield information on the nature of the contact discontinuity at $x = 0$. At the discontinuity $v_1 = v_2$ of course. Equation (2) implies $P_1 = P_2$, and the energy equation implies continuous heat flux across the discontinuity, so that the ratio of temperatures at a contact discontinuity is $T_2/T_1 = (m_1 Z_2 / m_2 Z_1)^{2/5}$, and the ratio of

densities in the quasi-steady state is $\rho_2/\rho_1 = (T_1/m_1)/(T_2/m_2) = (m_2/m_1)^{7/5}(Z_1/Z_2)^{2/5}$.

In the rest frame of the interface, the fluids I and II appear to be slowly compressed towards the interface on a characteristic time scale $T_1/m_1 g v_1$. For time scales much shorter than this, the solution to the fluid equations may be written

$$p \approx P_i\,[1 + \rho_i g x/P_i]\ ,\ \rho \approx \rho_i\,[1 + 3\rho_i g x/5P_i],\ v_x \approx v_y = 0. \qquad (9)$$

Thus over reasonable time scales the fluids I and II can be treated as incompressible. Equations (9) will be used as the basic, unperturbed state from which the stability analysis of the following section will proceed.

III. STABILITY ANALYSIS OF THE FLUID INTERFACE

Since the effects of heat conduction across the cold fluid interface in the unablated fluid are to be neglected, another equation is needed to close the system of fluid equations (1-3). We shall assume the perturbations are incompressible, adding the equation

$$\frac{\partial v_x}{\partial x} + \frac{\partial v_y}{\partial y} = 0\ . \qquad (10)$$

Since the basic state in (9) is independent of t and y, the perturbed quantities, after a Fourier decomposition, are proportional to $\exp(\gamma t + iky)$, in which k is the wave number in the y direction, and γ is the growth rate to be determined. Then linearizing the equations (1-3) and (10) yields the following equation for δv, the perturbed velocity in the x direction[5]

$$\frac{d}{dx}\left(\rho \frac{d}{dx}\delta v\right) - k^2\rho\delta v = \frac{gk^2}{\gamma^2}\left(\frac{d\rho}{dx}\right)\delta v \qquad (11)$$

with the jump conditions

$$\delta v_1 = \delta v_2 \quad \text{and}$$

$$\rho_2 \left(\frac{d}{dx}\,\delta v\right)_2 - \rho_1 \left(\frac{d}{dx}\,\delta v\right)_1 = \frac{gk^2}{\nu^2}\,(\rho_2 - \rho_1)\,\delta v_2 \tag{12}$$

If x_a and the width of the fluid I, as illustrated in Fig. 1, are much greater than k^{-1}, then the fluids can be treated as essentiallly semi-infinite. In that case the solution of (11) that satisfies the boundary conditions of vanishing δv at $\pm \infty$ is

$$\delta v = \begin{cases} a \exp(-\mu kx) & x \geq 0 \\ b \exp(+\mu kx) & x \leq 0 \end{cases}$$

The jump conditions (12) require the constants a and b to be equal, and give the following relation for the positive constant μ

$$\mu = \frac{kg}{\nu^2}\left(\frac{\rho_1 - \rho_2}{\rho_1 + \rho_2}\right) \tag{13}$$

But the basic state of (9) and the equation (11) imply a dispersion relation for μ in fluid II of

$$\mu^2 - \frac{3\rho_2 g}{5P_2 k}\,\mu - \left(1 + \frac{3\rho_2 g^2}{5P_2 \nu^2}\right) = 0 \tag{14}$$

The constant μ can be eliminated from (13) and (14) to give the growth rate ν of perturbations at the fluid interface as

$$\nu^2 = \frac{kg}{(1+\beta^2)^{\frac{1}{2}} + \beta}\left(\frac{\rho_1 - \rho_2}{\rho_1 + \rho_2}\right) \tag{15}$$

in which $\beta \equiv (3\rho_1 g/5P_1 k)/(\rho_1/\rho_2 - 1)$.

The constant β is proportional to the density gradient on either side of the fluid interface, and reduces the growth of the instability there. Thus the density gradient caused by the acceleration of the slab inhibits the instability caused by the acceleration.

IV. APPLICATION TO LASER-FUSION PELLET DESIGN

The theory developed in the preceding sections has important implications for the design of layered laser-driven targets, regardless of their geometry. In this section the calculations of the preceding sections will be generalized to apply to any number of stratified fluids. The growth rates found for a planar geometry may be applied to an imploding spherical shell as well by the prescription $k \rightarrow (\ell + \frac{1}{2})/R$, where R is the radius and ℓ is the degree of a spherical harmonic in a decomposition of the Rayleigh-Taylor perturbation. The correspondence is valid until spherical convergence effects near the origin can no longer be neglected, that is, until $(dR/dt)^2 \ll Rd^2R/dt^2$ is no longer satisfied.[24]

An important laser-fusion pellet design that has been receiving considerable attention lately involves a hollow deuterium-tritium pellet surrounded by a high-density, high-Z shell and a moderately dense material on the outside acting as an ablator. Very thin shells having this design have been claimed to have been imploded stably in numerical experiments[20-22] using laser energies of 10^5-10^6 J and long pulsewidths of 10^{-8}-10^{-7} s.

The dense layer between the ablator and fuel serves several functions. It shields the fuel from preheat by superthermal electrons and x-rays and also from heat conduction, so that the fuel can be maintained on a low adiabat after the initial shocks pass through. Moreover, the shocks are reduced in strength by the density step from dense layer to fuel. The reduced thermal conduction also prevents shell burn-through at higher energy densities.

A fluid is susceptible to Rayleigh-Taylor instability whereever the acceleration is in the same direction as a density gradient. For the pellets discussed above, growth of the perturbation is potentially greatest at the ablation surface and at the interface between the ablator and dense shell. The treatment in this paper of instability in the latter case suggests that the growth rate might be reduced if the jump in density from ablator to dense shell were accomplished in several steps in density rather than just one. That is, the simple, linear analysis of this paper suggests a pellet shell design consisting of a layer of D-T fuel frozen onto the inner surface of a very dense material such as uranium (which might be caused to generate additional energy by fission). Surrounding the densest layer would be layers of successively decreasing density ending with the relatively low density ablator on the outside. A target of this general configuration is shown schematically in Fig. 2.

For such a configuration much of the analysis presented in preceding sections can be used, but the boundary conditions need to be reconsidered. Suppose the laser target consists of n layers. For the purposes of this analysis, the ablator from its cold, left interface to its surface of maximum density may be considered a layer. This presumes a decoupling of possible instability at the ablation surface with instabilities in the cold fluid. Let the maximum density of the j^{th} layer at its right interface be denoted ρ_j, and the jump in density at that interface be denoted $\Delta\rho_j$, with $\Delta\rho_j < 0$ for all but the interface of the shell with the fuel. Also let P_j denote the (continuous) pressure of the interface between layers j and $j+1$, and d_j be the width of the j^{th} layer. If the Mach number and $\rho_j g d_j / P_j$ are both much less than 1 in all the layers, then the unperturbed density in the j^{th} layer increases linearly with a gradient $3\rho_j^2 g/5P_j$.

The velocity perturbation in the j^{th} layer satisfies the equation

$$\left[\frac{d^2}{dx^2} + \frac{3\rho_j g}{5P_j}\frac{d}{dx} - k^2\left(1 + \frac{3}{5}\rho_j g^2/P_j\gamma^2\right)\right]\delta v = 0. \qquad (16)$$

The general solution in the j^{th} layer is

$$\delta v = a_j \exp(u_j^+ kx) + b_j \exp(u_j^- kx)$$

in which a_j and b_j are constants to be determined from boundary conditions, and u_j^+ and u_j^- are the positive and negative roots of the indicial equation of (16)

$$u_j^{\pm} \equiv \pm \left[\left(1 + \frac{3\rho_j g}{10P_j k}\right)^2 + \frac{3\rho_j g}{5P_j k}\left(\frac{gk}{\gamma^2} - 1\right)\right]^{\frac{1}{2}} - \frac{3\rho_j g}{10P_j k} \quad . \tag{17}$$

The two boundary conditions at each interface, namely continuity of δv and of $\rho(d\delta v/dx) - gk^2\rho\delta v/\gamma^2$, together with one boundary condition on the left of the target and one on the right represent the 2n conditions that completely determine 2n-1 constants (one of the 2n constants a_j and b_j is arbitrary) and the growth rate γ.

By applying the two boundary conditions at each interface, the velocity perturbation in the ablator (n^{th} layer) can be related to the velocity perturbation in the fuel layer (first layer) by

$$\begin{pmatrix} a_n \\ b_n \end{pmatrix} = M^{(n-1)} \cdot M^{(n-2)} \cdots M^{(1)} \begin{pmatrix} a_1 \\ b_1 \end{pmatrix} \tag{18}$$

The 2x2 matrix $M^{(j)}$ has elements

$$M_{11}^{(j)} = \alpha_j^+ \exp[(u_j^+ - u_{j+1}^+)kx_j]$$

$$M_{12}^{(j)} = \alpha_j^- \exp[(u_j^- - u_{j+1}^+)kx_j]$$

$$M_{21}^{(j)} = (1 - \alpha_j^+) \exp[(u_j^+ - u_{j+1}^-)kx_j]$$

$$M_{22}^{(j)} = (1 - \alpha_j^-) \exp[(u_j^- - u_{j+1}^-)kx_j]$$

in which

$$\alpha_j^+ \equiv [\rho_j u_j^+ + (gk/\nu^2)\Delta\rho_j - (\rho_j + \Delta\rho_j)u_{j+1}^-]/[(\rho_j + \Delta\rho_j)(u_{j+1}^+ - u_{j+1}^-)]$$

$$\alpha_j^- \equiv [\rho_j u_j^- + (gk/\nu^2)\Delta\rho_j - (\rho_j + \Delta\rho_j)u_{j+1}^-]/[(\rho_j + \Delta\rho_j)(u_{j+1}^+ - u_{j+1}^-)]$$

and x_j is the position of the interface between layers j and j+1.

The ratios b_1/a_1 and a_n/b_n are fixed by right and left boundary conditions; a_1 can be chosen arbitarily; and (18) then represents two equations in the two unknowns b_n and ν. As a simple example, consider the two-layer problem of the previous section. For this case n = 2, and the boundary conditions imply $b_1 = a_2 = 0$. Then the two equations from (18) are $0 = M_{11}^{(1)} a_1$ and $b_2 = a_1$. The growth rate in (15) then follows after finding $u_1^+ = -u_2^-$.

The formal solution of the many-layer problem is subject to the same limitations of validity as the two-layer problem. However the formal solution presented in this section allows for any choice of boundary conditions at the rear face of the target and the ablation surface, and is therefore applicable to a target containing layers thinner than a perturbation wavelength as well as thicker.

To illustrate the stabilizing effect of interposing layers of intermediate density between layers of high and low density we present the following example. Consider two semi-infinite media of uniform densities ρ_1 and ρ_3 separated by a layer of uniform density ρ_2 and width d. This configuration is shown by the dashed lines in Fig. 3a. The growth rate is found from (18) in the zero-density-gradient limit to be

$$\frac{\nu^2}{gk} = \frac{(1-s)(r-1)(\omega-1)}{(r-s)\omega - \{(r-s)^2\omega^2 - (1-s)(r-1)[(1+rs)(\omega-1)^2 + (r+s)(\omega^2-1)]\}^{\frac{1}{2}}}$$

in which $r \equiv \rho_1/\rho_2$, $s \equiv \rho_3/\rho_2$, and $\omega \equiv \exp(2kd)$.

For slabs of uniform density, the optimal reduction in growth occurs when the intermediate density is the geometric mean of the upper and lower densities, or $rs = 1$. In that case the growth rate can be reduced by a factor of as much as $(r^2 + 1)^{\frac{1}{2}}/(r + 1)$, depending on the intermediate slab width. The growth rate is plotted versus intermediate slab width as a dashed curve in Fig. 3b for the case $\rho_1 = 2\rho_2 = 4\rho_3$.

But now suppose that the density gradients caused by the acceleration are high. For example let $d\ln\rho/dx = k$ for $x < 0$. Then the growth rate for the configuration shown by the solid curve in Fig. 3a is given by the solid curve in Fig. 3b.

Several features of Fig. 3 should be noted. Most important is that a layer of intermediate density reduces the growth rate at an unstable fluid interface. The stabilizing effect of the intermediate layer saturates at a width greater than about k^{-1} as expected, since treating slabs of width greater than about k^{-1} as semi-infinite is known to be a good approximation. The density gradients established in the fluid by the acceleration stabilize the fluid interfaces even further, and intermediate-density layers are even more effective in reducing the growth rate when the density gradient in the unablated fluid is high. The density gradient in steady state, $\partial\rho^2 g/\partial P$, is high for fluids of high density and low temperature.

This example illustrates the effectiveness of intermediate-density layers and natural acceleration-induced density gradients in reducing the Rayleigh-Taylor instability at material interfaces in laser-driven targets.

The stabilizing effect of the density gradients can be enhanced by creating steeper artifical density gradients in the basic state of the slab on either side of material discontinuities. This can be accomplished by creating the layers with continuous blends of materials rather than of one material only. In practice such inhomogeneous layers

might be fabricated by condensing two gases onto the pellet surface simultaneously at controlled rates. The growth rate of the instability of such an inhomogeneous pellet can be calculated by replacing the logarithmic density gradient $\partial\rho_j g/\partial P$ in (16) and (17) by the appropriate values, and following the same procedure as before.

V. CONCLUSIONS

Growth of the Rayleigh-Taylor instability, particularly long wavelength perturbations, at a fluid interface in a laser-driven target is inhibited naturally by the density gradients produced by the acceleration of the fluid. Within certain limits of validity, the growth rate for any number of stratified layers of materials in a laser-driven target has been expressed in closed form. It is found that interposing a layer of intermediate density reduces the instability further, and most effectively if the intermediate density is the geometric mean of the high and low densities. Even greater advantage can be gained by fabricating the target layers with favorable density gradients between the discontinuities.

It is important to understand the roles of stabilizing mechanisms at fluid interfaces, because inhomogeneous laser targets offer many advantages and present good prospects for successful laser-induced fusion schemes.

I wish to thank S. E. Bodner and D. L. Book for valuable comments and advice.

REFERENCES

1. G. I. Taylor, Proc. Roy. Soc. (London) A201, 192 (1950).
2. F. H. Harlow and J. E. Welch, Phys. Fluids 9, 842 (1966).
3. R. E. Kidder in Proceedings of Japan-U.S. Seminar on Laser Interaction with Matter, ed. by C. Yamanaka (Tokyo International Book Co., Tokyo, 1975); K. Lee, et al., Phys. Fluids 20, 51 (1977).
4. F. S. Felber, Phys. Rev. Lett 39, 84 (1977).
5. S. Chandrasekhar, Hydrodynamic and Hydromagnetic Stability (Clarendon, 1961).
6. B. R. Morton, Quart. J. Mech. Appl. Math. 10, 433 (1957); K. A. Brueckner and S. Jorna, J. Plasma Physics 16, 285 (1976).
7. S. E. Bodner, Phys. Rev. Lett. 33, 761 (1974).
8. R. D. Richtmyer, Commun. Pure Appl. Math. 13, 297 (1960).
9. J. P. Boris, Comments on Plasma Physics and Controlled Fusion, to be published; NRL Memo Report 3427 (1977); Bull. Am. Phys. Soc. 21, 1103 (1976).
10. J. D. Lindl, et al., Bull. Am. Phys. Soc. 21, 1103 (1976).
11. R. E. Kidder, Nuc. Fusion 16, 3 (1976).
12. J. D. Lindl and W. C. Mead, Phys. Rev. Lett. 34, 1273 (1975).
13. J. N. Shiau, E. B. Goldman, and C. I. Weng, Phys. Rev. Lett. 32, 352 (1974).
14. D. B. Henderson, R. L. McCrory and R. L. Morse, Phys. Rev. Lett. 33, 205 (1974).
15. K. A. Brueckner, S. Jorna, and R. Janda, Phys. Fluids 17, 1554 (1974).
16. J. Nuckolls, et al., Fifth IAEA Conference on Plasma Physics and CTR, 535 (Nov. 1974).
17. G. S. Fraley, et al., Fifth IAEA Conference on Plasma Physics and CTR, 543 (Nov. 1974).
18. R. J. Mason and R. L. Morse, Phys. Fluids 18, 814 (1975).
19. G. S. Fraley, Phys. Fluids 19, 1495 (1976).
20. Yu. V. Afanas'ev et al., JETP Lett. 21, 68 (1975).

21. Yu. V. Afanas'ev, et al., Priroda 10, 4 (1976).
22. Yu. V. Afanas'ev, et al., to be published.
23. L. Spitzer, Jr., Physics of Fully Ionized Gases (Interscience, N.Y., 1962), p. 144.
24. M. S. Plesset, Jour. Appl. Phys. 25, 96 (1954).

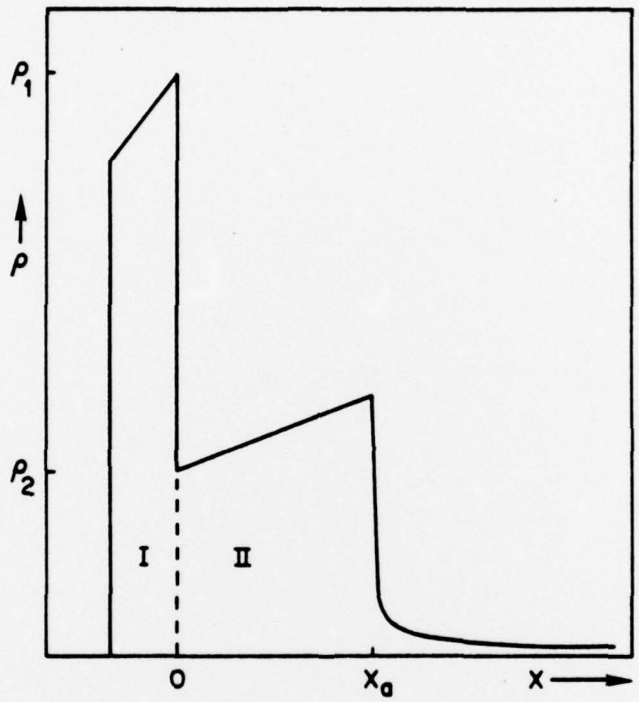

Fig. 1 — Quasi-steady density profile of inhomogeneous laser-driven target in accelerating rest frame of ablation surface at x_a. Fluid II is accelerating denser fluid I to left. Upper and lower densities at contact discontinuity are ρ_1 and ρ_2.

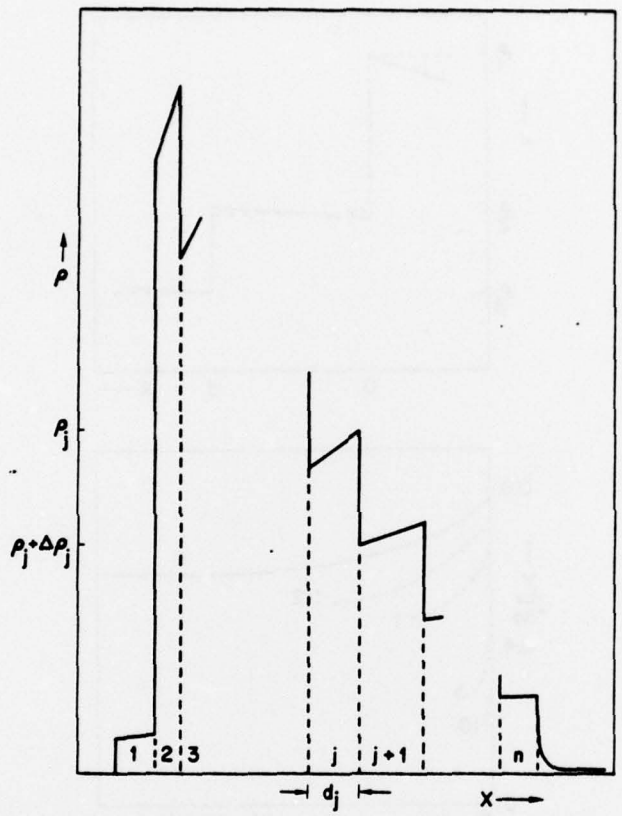

Fig. 2 — Schematic quasi-steady density profile of layered, inhomogeneous, laser-driven target consisting of n strata of distinct fluids. Jump in density from layer j to j+1 is $\Delta\rho_j$.

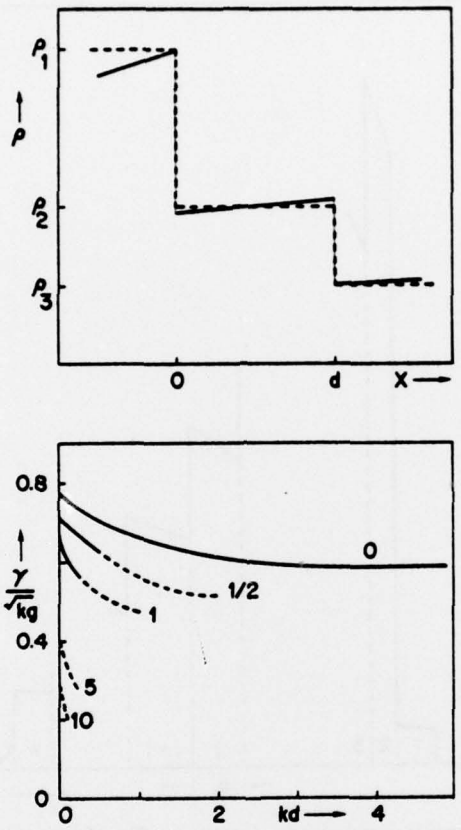

Fig. 3 — (a) Solid curve is density profile of two 'semi-infinite' layers separated by intermediate layer of width d; density gradients are produced by acceleration of system to left. Dashed curve is same configuration in limit of zero density gradients. (b) Rayleigh-Taylor growth rates in units $(kg)^{1/2}$ versus intermediate slab width in units k^{-1} of the corresponding density configurations in (a) for the case $\rho_1 = 2\rho_2 = 4\rho_3$. Solid curve gives growth rate for the mode $k = d \ln\rho_1/dx$; dashed curve corresponds to the large wavenumber (uniform density) limit.